Numerical Prediction of the Aerodynamic Noise From the Ducted Tail Rotor

Na Guo

Abstract—**In this paper, a numerical study into the unsteady aerodynamic performance of a ducted tail rotor based on CFD technique is presented. Computation was carried out for ideal forward flight condition. The general governing equations of turbulent flow around ducted tail rotor are given, and directly solved by using finite volume discretization and Runge-Kutta time integration. In order to predict the aerodynamic noise, a hybrid method combing computational aeroacoustic with boundary element method (BEM) has been proposed. The unsteady flow around rotors is calculated using the CFD method to get the noise source information. The radiate sound pressure is calculated using the acoustic analogy FW-H equation in the frequency domain. The scattering effect of the duct wall on the propagation of the sound wave is presented using the BEM. The results are validated against existing technique. The sound pressure directivity and scattering effect are shown to demonstrate the applicability and validity of the approach.**

Index Terms—**Ducted tail rotor, Aerodynamic performance, Aerodynamic noise, Boundary element method**

I. Introduction

With the development of helicopter technology, its noise level has become one of substantial indexes of helicopter characteristic [1-5]. Helicopter tail rotor is a major noise source, therefore investigation of tail rotor noise characteristic becomes much valuable and important to control the helicopter noise level. For single main rotor helicopter usually a tail rotor is used to provide the necessary anti-torque and control around the yaw axis. For this reason, conventional tail rotor or ducted tail rotor can be applied. In recent years, the analysis of the tail rotor has been one of the research priorities in the field of helicopter technology [6-8].

In contrast to the conventional configuration, the containing shroud of a ducted tail rotor provides peripheral protection and acts as an acoustic shield. Compared to the open tail rotor, the ducted tail rotor is characterized by a higher number of blades that rotate at higher speed. Typically, both the duct and rotors of the ducted tail rotor can generate thrust. Thrust which is produced by the duct is due to negative pressure on the duct inlet, which contributes maximum 50% to the total. In addition, the noise of ducted tail rotor is lower than the conventional open-type rotor [9-10]. Therefore, the analysis of the aerodynamic noise of the ducted tail rotor is the main purpose of the paper.

Aerodynamic characteristics of the ducted tail rotor should be obtained firstly to predict the aerodynamic noise. Along with the development of the ducted tail rotor, many researchers have studied the aerodynamic characteristics of various types of ducted tail rotors [11-13]. The main method which investigates the aerodynamic performance of ducted tail rotor is CFD (Computational Fluid Dynamic) technique. Among those CFD techniques, momentum source method is one of the commonly used methods. The momentum source with functional relationship to the local flow conditions represents the spanning rotor in flow field and are added to the N-S equations by UDF procedure. Song et.al. [15] used it to analysis the aerodynamic characteristics of ducted tail rotor. Cao and Yu [14] applied it to solve the numerical simulation of turbulent flow around ducted tail rotor. Even though momentum source method is quite successful for the prediction of the aerodynamic performance of ducted tail rotor, detailed three dimensional flow features cannot be accurately predicted. Due to the approximation of the blade shape parameters, the accuracy of the momentum source method is still limited. In addition, it is difficult to acquire the accurate noise source information by using the momentum source method. In this work, a CFD technique which is considered the blade shape parameters has been proposed to investigate the aerodynamic characteristics of ducted tail rotor, and the method is based on moving reference frame (MRF) model.

Calculation of the acoustic field radiated by rotating sources is a meaningful problem in the prediction of the helicopters noise. The main techniques for noise prediction are based on acoustic analogy Ffowcs Williams-Hawkings (FW-H) equation and the generalized treatment of Goldstein [16-18]. The established FW-H equation divides the aeroacoustic source into three types: monopole source, dipole source and quadrupole source. Although the aerodynamic characteristics of ducted tail rotor have been discussed by many researchers [19, 20], the investigation of the aerodynamic noise is relatively few. The prediction of rotating blade aerodynamic noise can be obtained easily by solving acoustic analogy FW-H equation, but the scattering effect of the duct wall on the propagation of the sound wave is difficult to discuss and the scattering mechanism is rather complex. Based on these problems, a boundary element method is developed to consider the scattering effect of the solid wall in the present study and to predict the far-field aerodynamic noise of the ducted tail rotor. The BEM is derived from boundary integral equation involving the surface pressure and normal acoustic velocity at the boundary of the acoustic domain. The directivity of the sound pressure is also shown in this research.

Manuscript received August 7, 2017; revised January 16, 2018.

Na Guo (Corresponding author) is with the Institute of Disaster Prevention, Sanhe, Hebei, P.R.China (e-mail: naguo8899@163.com).

II. GOVERNING EQUATIONS

The compressible, three dimensional Euler equations are expressed as in an integral form on rotational frame of reference using absolute flow variables:

$$\frac{\partial}{\partial t}\int_{\Omega}\hat{Q}d\Omega+\int_{\partial\Omega}F(\hat{Q},n)dS=\int_{\Omega}S(\hat{Q})d\Omega \tag{1}$$

where $\hat{Q}=\begin{pmatrix}\rho_0\\ \rho_0 u\\ \rho_0 v\\ \rho_0 w\\ e_0\end{pmatrix}$, $F(\hat{Q},n)=\begin{pmatrix}\rho_0 U_r\\ \rho_0 u U_r+\tilde{p}n_x\\ \rho_0 v U_r+\tilde{p}n_y\\ \rho_0 w U_r+\tilde{p}n_z\\ e_0 U_r+\tilde{p}U\end{pmatrix}$,

$S=\begin{pmatrix}0\\ \omega\rho_0 v\\ -\omega\rho_0 u\\ 0\\ 0\end{pmatrix}$, U_r is the normal component of the relative velocity on the rotational frame, u, v and w are the Cartesian components in inertial frame. n_x, n_y and n_z are the Cartesian components of the exterior surface unit normal vector on $\partial\Omega$. ρ_0 is the static density of fluid without acoustic disturbance, $\tilde{p}$ denotes fluid pressure. All parameters are normalized by freestream speed of sound, freestream density and blade chord length.

Eq.(1) is discretized by using Jameson cell-centered finite volume method. Inviscid flux across each cell face is calculated applying Roe's flux-difference splitting formula. An explicit time integration algorithm based on the multistep Runge-Kutta is used to advance the solution in time. The linear system obtained by using above method is solved by applying Gauss-Seidel method. The standard $k-\varepsilon$ model is adopted here because of its reasonable accuracy and fewer resources. The moving reference frame is also used to solve the problem of rotating. The inlet condition is set to the velocity-inlet. In order to accelerate the convergence, a local time step and implicit residue smoothing have been used. The detailed procedure for solving the governing equations can be found in Ref.[21].

III. COMPUTATIONAL METHOD OF ACOUSTIC NOISE

FW-H aeroacoustic analogy method is used to investigate the generation of the aerodynamic noise. The general equation is given by

$$\left(\frac{1}{c_0^2}\frac{\partial}{\partial t^2}-\frac{\partial^2}{\partial x_i^2}\right)p'(x,t)=\frac{\partial}{\partial t}\left[\rho_0 v_n\delta(f)\right]-\frac{\partial}{\partial x_i}\left[P_{ij}n_j\delta(f)\right]+\frac{\partial^2}{\partial x_i\partial x_j}\left[T_{ij}H(f)\right] \tag{2}$$

where c_0 is the speed of sound, v_n is the normal component of the surface velocity, p' is the acoustic pressure. n_j is the unit normal vector pointing toward the exterior region. $\delta(f)$ and $H(f)$ are Dirac delta function and Heaviside function. f is a moving Kirchhoff surface. The terms on the right hand side of Eq.(2) are interpreted as source terms. $\partial\left[\rho_0 v_n\delta(f)\right]/\partial t$ denotes the monopole source. P_{ij} is the compressive stress tensor, $-\partial\left[P_{ij}n_j\delta(f)\right]/\partial x_i$ denotes the dipole source. T_{ij} is the Lighthill stress tensor, $\partial^2[T_{ij}H(f)]/\partial x_i\partial x_j$ denotes the quadrupole source.

After the CFD calculation, the aerodynamic noise at observation point is calculated using the FW-H equation by referring to the time history of the blade loading of the CFD results. The quadrupole source is neglected because the noise of the ducted tail rotor in hover is mainly generated by the monopole source and dipole source. Therefore Eq.(2) can be reduced to

$$\left(\frac{1}{c^2}\frac{\partial}{\partial t^2}-\frac{\partial^2}{\partial x_i^2}\right)p'(x,t)=\frac{\partial}{\partial t}\left[\rho_0 v_n\delta(f)\right]-\frac{\partial}{\partial x_i}\left[P_{ij}n_j\delta(f)\right] \tag{3}$$

The solution of Eq.(3), the formulation of Farassat 1A, is expressed as

$$p'(x,t)=p'_T(x,t)+p'_L(x,t) \tag{4}$$

with

$$4\pi p'_T(x,t)=\int_S\left[\frac{\rho_0\dot{v}_n}{r(1-M_r)^2}\right]_{ret}dS+\int_S\left[\frac{\rho_0 v_n(r\dot{M}_i\hat{r}_i+c_0M_r-c_0M^2)}{r^2(1-M_r)^3}\right]_{ret}dS \tag{5}$$

$$4\pi p'_L(x,t)=\frac{1}{c_0}\int_S\left[\frac{\dot{l}_i\hat{r}_i}{r(1-M_r)^2}\right]_{ret}dS+\int_S\left[\frac{l_r-l_iM_i}{r^2(1-M_r)^2}\right]_{ret}dS+\frac{1}{c_0}\int_S\left[\frac{l_r(r\dot{M}_i\hat{r}_i+c_0M_r-c_0M^2)}{r^2(1-M_r)^3}\right]_{ret}dS \tag{6}$$

where $p'_T(x,t)$ is called thickness noise, $p'_L(x,t)$ is called loading noise. A detail description and the validation of the parameters are shown in Ref.[22].

IV. BOUNDARY ELEMENT METHOD FOR FAR-FIELD ACOUSTIC RESPONSE

A. Boundary element formulation

In a homogeneous medium, for three dimensional linear time harmonic problem of the external acoustics with Neumann Boundary Condition (Shown in Fig.1), the solution of the Helmholtz equation is [23,24]

$$C(P)p(P)=\int_S\left(\frac{\partial G(Q,P)}{\partial n}p(Q)-G(Q,P)\frac{\partial p(Q)}{\partial n}\right)dS(Q) \tag{7}$$

where

$$C(P)=\begin{cases}1 & P\in B'\\ \frac{1}{2} & P\in S \text{ and } S \text{ is smooth boundary}\\ 1-\int_S\frac{\cos\beta}{4\pi r^2}dS(Q) & P\in S \text{ and } S \text{ is nonsmooth boundary}\\ 0 & P\notin(S\cup B')\end{cases} \tag{8}$$

where P is a general field point, Q is the source point, p is the acoustic pressure, B' stands for the domain of the propagation, S is the boundary of B', n is the unit normal at $Q \in S$ and directed into B'. $G(r) = -e^{ikr}/4\pi$ is the Green function in the free space, and $r = \|P - Q\|_2$. β is angle between n and r.

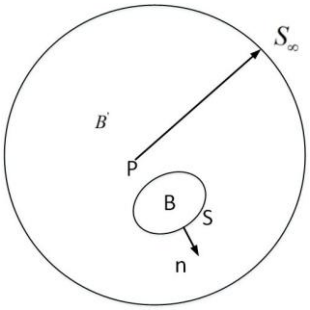

Fig.1 External acoustics problem

B. Numerical discretization

In order to obtain solution of Eq.(7), boundary S should be divided into N quadrilateral elements ($S = \sum_{j=1}^{N} S_j$). Then Eq.(7) can be discretized as a linear algebra system. After applying the relationship between the fluid normal velocity and acoustic pressure $\frac{\partial p(Q)}{\partial n} = -i\omega\rho_0 v_n(Q)$ and $\frac{\partial G(Q,P)}{\partial n} = -\frac{e^{-ikr}}{4\pi r}(ik + \frac{1}{r})\cos\beta$, for any observation points P defined by the node i, the Eq.(7) can be transformed into

$$c_i p_i = \sum_{j=1}^{N} \int_{S_j} p_j(Q) \frac{\partial G(Q, P_i)}{\partial n} dS + i\rho_0\omega \sum_{j=1}^{N} \int_{S_j} v_j(Q) G(Q, P_i) dS \tag{9}$$

For each j, the pressure $p_j(Q)$ and the normal velocity $v_j(Q)$ can be discretized as a function of their nodal values

$$p_j(Q) = \sum_{k=1}^{4} N_k p_{j,k} = \boldsymbol{N}\boldsymbol{p}_j \tag{10}$$

$$v_j(Q) = \sum_{k=1}^{4} N_k v_{j,k} = \boldsymbol{N}\boldsymbol{v}_j \tag{11}$$

where N_k denote basis functions, for the quadrilateral elements, N_k can be written as

$$N_1 = \frac{1}{4}(1-\xi_1)(1-\xi_2) \tag{12a}$$

$$N_2 = \frac{1}{4}(1+\xi_1)(1-\xi_2) \tag{12b}$$

$$N_3 = \frac{1}{4}(1+\xi_1)(1+\xi_2) \tag{12c}$$

$$N_4 = \frac{1}{4}(1-\xi_1)(1+\xi_2) \tag{12d}$$

Then Eq.(9) becomes

$$c_i p_i = \sum_{j=1}^{N}\sum_{k=1}^{4} p_{j,k} \int_{S_j} N_k \frac{\partial G(Q_j, P_i)}{\partial n} dS + i\rho_0\omega \sum_{j=1}^{N}\sum_{k=1}^{4} v_{j,k} \int_{S_j} N_k G(Q_j, P_i) dS \tag{13}$$

or the following

$$c_i p_i = \sum_{j=1}^{N}\sum_{k=1}^{4} p_{j,k} H_{ij,k} + i\rho_0\omega \sum_{j=1}^{N}\sum_{k=1}^{4} v_{j,k} G_{ij,k} \tag{14}$$

where

$$H_{ij,k} = \int_{S_j} N_k \frac{\partial G(Q_j, P_i)}{\partial n} dS \tag{15}$$

$$G_{ij,k} = \int_{S_j} N_k G(Q_j, P_i) dS \tag{16}$$

Taking place of the points P_i by the boundary Q_j, we can get

$$c_i \delta_{ij} p_j = \sum_{j=1}^{N}\sum_{k=1}^{4} p_{j,k} H_{ij,k} + i\rho_0\omega \sum_{j=1}^{N}\sum_{k=1}^{4} v_{j,k} G_{ij,k} \tag{17}$$

When the procedure is repeated for the all points N of boundary element mesh, a linear algebra system can be obtained as follows

$$\boldsymbol{H}\boldsymbol{p} = i\rho_0\omega\boldsymbol{G}\boldsymbol{v} \tag{18}$$

where $\boldsymbol{p}$ and $\boldsymbol{v}$ denote the sound pressure and velocity in the normal direction to the surface at the nodal points of the boundary element mesh. Once the sound pressure on the boundary is known, the pressure at any point in the exterior sound field can be determined by Eq.(13), at this moment, $P_i \in B'$.

In Eq.(17), when the source point coincides with a filed point, Eq.(15) and Eq.(16) become singular integral. These singular integrals can be solved by many methods, in this paper, we adopt a kind of coordinate transformation method. More details can be obtained in Ref.[25].

V. Numerical Results and Discussions

A. Geometric configuration and mesh generation

To demonstrate the effectiveness of the present method, we consider a model of ducted tail rotor at TsAGI, which has been installed on the Ka-60 helicopter. Fig.2 shows CATIA geometric model of TsAGI ducted tail rotor. Its geometric dimensions are tabulated in Table I as reported in Ref.[26].

A structured mesh is generated around the duct of the TsAGI model, and the surface quadrilateral for the all configuration is presented in Fig. 3. The tail rotor of the TsAGI model is meshed with an unstructured mesh which is shown in Fig.4, and an adaptive encryption technique is adopted to mesh the leading edge and the trailing edge of the tail rotor.

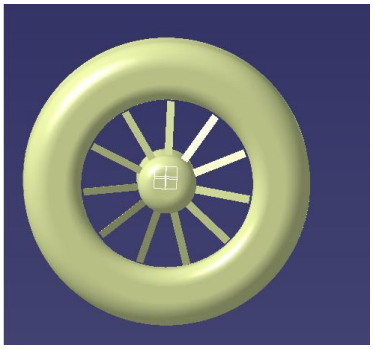

Fig.2 geometric model of TsAGI ducted tail rotor

Table I.
Geometric dimensions of the ducted tail rotor

Rotor	Radius	297mm
	Number of blades	11
	Solidity	0.4951
	Twist angle	-12deg
	Tip speed	74.6m/s
	Airfoil	NACA23012 (r/R=0.35~1.0)
Duct	Tip clearance gap	0.01R
	Inlet radius	0.2R
	Diffuser length	0.7R
	Diffuser angle	4 degrees

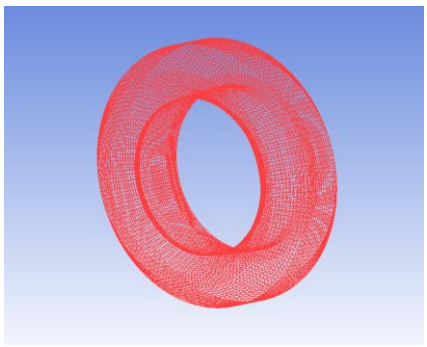

Fig.3 Surface quadrilateral for the duct

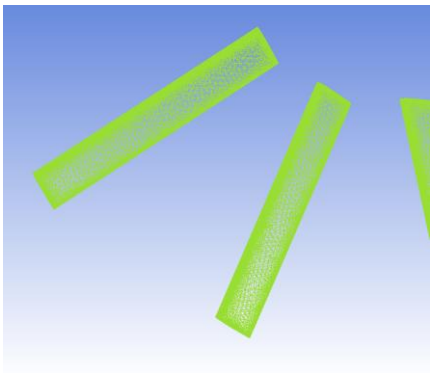

Fig.4 Surface quadrilateral for the tail rotor

B. *Aerodynamic performance of the ducted tail rotor*

An initial condition is made for the ducted rail rotor at a tip mach number of 0.22 and a collective pitch angle of 40degree at the blade root. At this moment, the rotor produces thrust equivalent to 9.547kg. The rotor thrust in the Ref.[27] and Ref.[28] were 9.54kg and 9.69kg respectively. The coincidence indicates that our method can investigate aerodynamic performance of ducted tail rotor effectively. The predicted sectional thrust distribution along the rotor in Fig.5 is also compared with the momentum source theory and the vortex theory [26], which shows a good agreement.

The predicted hover flow filed is expressed as streamlines in Fig.6 for X=0 cutting plane in the axial direction. From the Fig.6, we can find that two vertexes appear at each side of the duct outlet under the influence of outlet flow and also two vertexes exist below the center body. Flow separation at the base of center body is obvious in Fig.6.

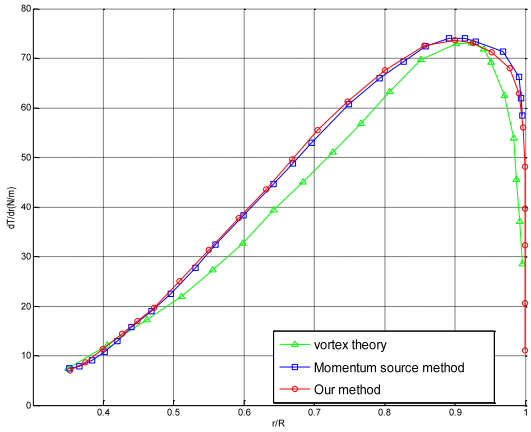

Fig.5 Comparison of the spanwise distribution of the blade loading.

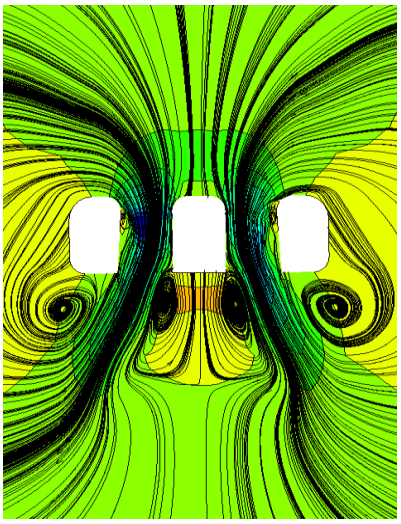

Fig.6 Hover streamlines for X=0 cutting plane in the axial direction

C. *Aerodynamic noise of the ducted tail rotor*

Through the analysis of aerodynamic performance of TsAGI ducted tail rotor, we can acquire the unsteady flow properties and the enough pressure data of the surface of the rotor. Then they are transformed into data in frequency domain by applying fast Fourier transform method. The far-filed sound pressure is calculated using FW-H analogy in the frequency domain. Before using the BEM method to study the radiation and propagation of the sound source, we should use a simplified configuration which is shown in Fig.7 to consider the scattering effect of the duct. From the Fig. 7, we know that the surface is constructed by quadrilateral mesh. The maximum size of the mesh is 0.012m and the number of elements is 5107. In this section, we use a point force method which regarding the rotors as a series of points to investigate the scattering effect of the duct. The method can be applied in the prediction of the noise when the force fluctuations of the rotors are obtained.

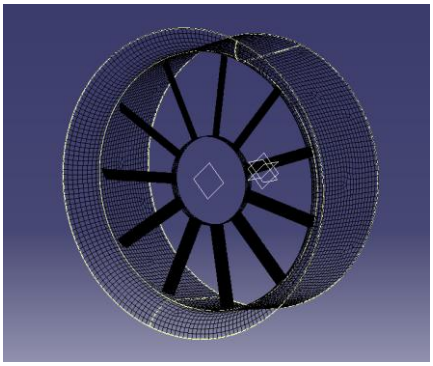

Fig.7 Mesh of duct used in BEM.

The sound pressure is expressed as dB (decibels) and the predicted SPL (sound pressure levels) is given by

$$SPL = 20\lg\frac{P_e}{P_r} \tag{19}$$

where P_e denotes the predicted pressure, P_r denotes the reference pressure and equal to 2×10^{-5}Pa.

The comparisons of the directivity of SPLs between the tail rotor without duct and the ducted tail rotor are shown in Fig.9 and Fig.10. The observation distance in Fig.9 and Fig.10 are 5R and 20R respectively. From the Fig.9 and Fig.10, we can conclude that the SPLs of the ducted tail rotor are smaller than the tail rotor without duct, and the SPL attenuation with distance is normally stronger than that of the tail rotor without duct. We also see that the scattering effect of the duct wall can change the sum sound pressure.

The directivity of SPLs for various observation distance is presented in Fig.11. From the Fig.11, we can find that the SPLs become smaller and smaller when the observation distance increases.

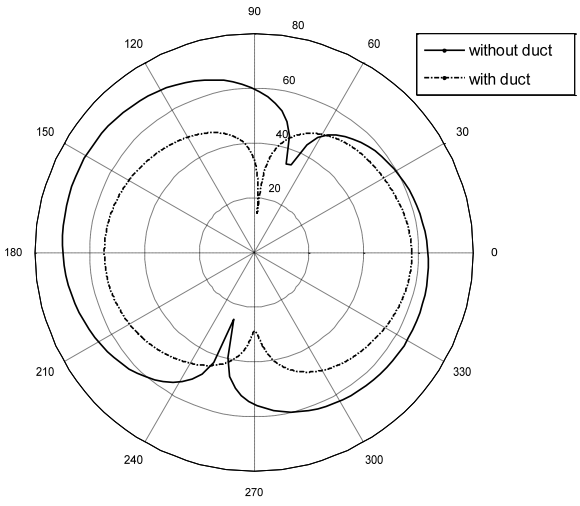

Fig.9 Directivity of SPLs between the tail rotor without duct and the ducted tail rotor at 5R distance

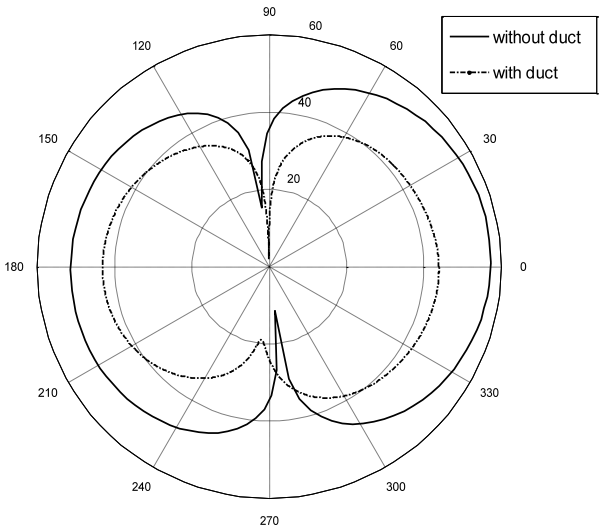

Fig.10 Directivity of SPLs between the tail rotor without duct and the ducted tail rotor at 20R distance

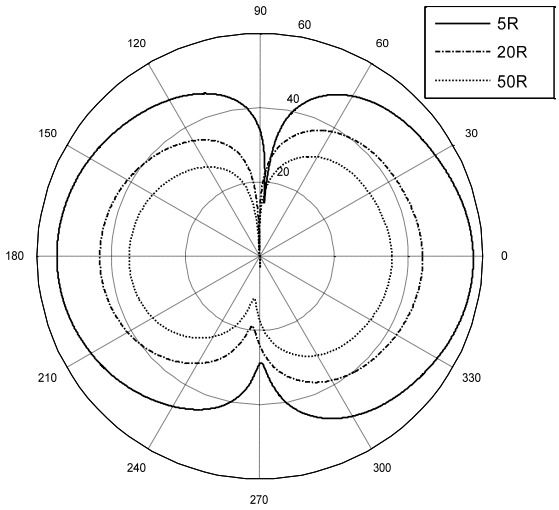

Fig.11 Directivity of SPLs of the ducted tail rotor at different distance.

VI. Conclusion

The aim of this paper is to develop an effective method for predicting the aerodynamic noise of the ducted tail rotor in hover numerically. A CFD method based on MRF model is used to study the aerodynamic performance of ducted tail rotor. Calculations are made for TsAGI ducted tail rotor, and the results are compared with vortex theory and momentum source method for validation. The unsteady blade force is also obtained and transferred to the FW-H analogy to calculate the sound source without the duct. In order to consider the scattering effect of the duct, a BEM is proposed to predict the far-filed aerodynamic noise. The numerical results show that the scattering effect of the duct should be included in the prediction of the noise. They also indicate that the SPLs of the ducted rotor are lower than that of the open-type tail rotor, and their attenuation is stronger. The control of the inlet noise is advisable for the ducted tail rotor noise reduction.

REFERENCES

[1] P. Cyril, Z. Joelle, R. Olivier, et al, "Helicopter Rotor Noise Prediction Using ONERA and DLR Euler / Kirchhoff Methods," *Journal of the AHS*, vol.44, no.2, pp. 121-131, 1999.

[2] I. I. Lázaro, A. Álvarez, et al, "The identification problem applied to periodic systems using Hartley series," *Engineering Letters*, vol. 21, no. 1, pp. 36-43, 2013.

[3] A. Desopper, P. Lafon, J. J. Philippe, J. Prieur, "Effect of an Anhedral Sweptback Tip on the Performance of a Helicopter Rotor," *Vertica*, vol.12, no.4, pp. 345-355, 1988.

[4] W. Johnson, *Helicopter Theory*. Princeton University Press 1980.

[5] A. R. George , "Helicopter Noise: State-of-the-Art," *Journal of Aircraft*, vol.15, no.11, pp. 707-715, 1978.

[6] R. Mouille, "The Fenestron, Shrouded Tail Rotor of the SA341 Gazelle," *Journal of the American Helicopter Society*, vol.15, no.4, pp.31-37, 1970.

[7] T. Taniguchi, M. Sugeno, "Trajectory tracking controls for non-holonomic systems using dynamic feedback linearization based on piecewise multi-linear models," *IAENG International Journal of Applied Mathematics*, vol. 47, no. 3, pp. 339-351, 2017.

[8] R. Mouille, F. Morelli, "New Aerodynamic Design of the Fenestron for Improved Performance," *Proceedings of the 12th European Rotorcraft Forum*, 1986.

[9] C. Keys, M. Sheffler, S. Weiner, et al. , "LH Wind Tunnel Testing: Key to Advanced Aerodynamic Design," *the 47th Annual Forum of American Helicopter Society*, Phoenix, pp.77-87, 1991.

[10] R. A. Desjardins, W. L. Noehren, A. N. Bertolazzi, "Design and Flight Test Evaluation of the FantailTM Antitorque System," *the 47th Annual Forum of American Helicopter Society*, Phoenix,:pp. 857-867, 1991.

[11] R. G. Rajagopalan, C. N. Keys, "Detailed aerodynamic analysis of the RAH-66 FANTAIL using CFD," *J. Am. Helicopter Soc.*, vol.42, pp. 310-320, 1997

[12] S. Bandoh, M. Fudamoto, T. Akiyama, "The ducted tail rotor system of the New Observation (XOH-1)," *Proc. AHS International Meeting on Advanced Rotorcraft Technology and Disaster Relief*, Gifu, Japan, 1998.

[13] A. Vuillet, F. Morelli, "New aerodynamic design of the Fenestron for improved performance," *Proc. 12th European Rotorcraft Forum*, 1986.

[14] Y. H. Cao, Z.W. Yu, "Numerical simulation of turbulent flow around helicopter ducted tail rotor," *Aerospace Science and Technology*, vol.9, pp. 300-306, 2005.

[15] C.H. Song, Y.F. Lin, W.X. Chen, Y. T.Liu, "CFD analysis for the ducted tail rotor based on momentum source method," *Helicopter Technique*, vol.1, pp. 6-11, 2009.

[16] J. E. Ffowcs Williams, D. L. Hawkings, "Sound Generated by Turbulence and Surfaces in Arbitrary Motion," *Philosophical Transactions of the Royal Society*, vol. A264, no.1151, pp.321-342, 1969.

[17] F. Farassat, K. S. Brentner, "The Uses and Abuses of the Acoustic Analogy in Helicopter Rotor Noise Prediction," *Journal of the AHS*, vol.33, no.1, pp.29-36, 1988.

[18] F. Farassat, K. S. Brentner, "Supersonic Quadrupole Noise Theory for High-Speed Helicopter Rotors," *Journal of Sound and Vibration*, vol. 218, no.3, pp.481-500, 1998.

[19] Y. H. Cao, K.. Chen , J. Wang ," Analysis on ducted tail rotor and airfoil aerodynamic characteristics with CFD," *Aircraft Engineering and Aerospace Technology*, vol.77, no.1, pp. 62-67, 2005.

[20] Z. W. Yu, Y. H. Cao, "CFD Simulation and Validation of Ducted Tail Rotor," *Journal of Aerospace Power*, vol.21, no.1, pp. 19-24, 2006.

[21] Y. H. Cao, J. Wang, J. Su, "Mixed Jameson/total-variation-diminishing scheme applied to simulating rotor airfoil flow field," *AIAA Journal of Aircraft*, vol.40, no.1,pp. 213-216, 2003.

[22] K. S. Brentner, "Prediction of helicopter rotor noise-a computer program incorporating realistic blade motions and advanced formulation," NASA TM 87721, 1986.

[23] S. Qu, S. Li, H. R. Chen, Z. Qu, "Radial integration boundary element method for acoustic eigenvalue problems," *Engineering Analysis with Boundary Elements*, vol.37, pp. 1043-1051, 2013.

[24] Y. S. Wei, Y. S. Wang, S. P. Chang, J. Fu, "Numerical prediction of propeller excited acoustic response of submarine structure based on CFD, FEM and BEM," *Journal of Hydrodynamics*, vol.24, no.2, pp. 207-216, 2012.

[25] Z. G. Zhao, Q. B. Huang, "Calculation of singular integral for Helmholtz Boundary Integral Equation in Acoustics," *Chinese Journal of engineering mathematics*, vol.21, no.5, pp. 779-784, 2004.

[26] B. N..Bourtsev, S.V. Selemenev, "Fan-in-Fin performance at hover computational method," *Proc. 26th European Rotorcraft Forum*, 2000.

[27] W. R. Tan, S. L. Huang, G.H. Xu, "Analysis on aerodynamics characteristics of helicopter ducted tail rotor," *the 3th science and technology society of Chinese aviation*, pp. 204-210.

[28] H. D. Lee, O. J. Kown, J. Joo, "Aerodynamic performance analysis of a helicopter shrouded tail rotor using an unstructured mesh flow solver," *the 5th Asian Computational Fluid Dynamics Forum*, 2003.